RSC Applied Polymers

Accepted Manuscript

This article can be cited before page numbers have been issued, to do this please use: Q. Li, D. Wang, T. Wang, Y. Zhang, S. Liu, S. Zhang, Z. Hu, L. Li, G. Wang and Y. Zhao, *RSC Appl. Polym.*, 2025, DOI: 10.1039/D5LP00144G.

ROYAL SOCIETY OF CHEMISTRY

rsc.li/RSCApplPolym

View Article Online
DOI: 10.1039/D5LP00144G

ARTICLE

Reversible B–O Bonds-Based Epoxy Vitrimer with High Thermo-Mechanical and Dynamic Properties Enhanced by Intermolecular B–N Coordination

Received 00th January 20xx,
Accepted 00th January 20xx

DOI: 10.1039/x0xx00000x

Qi Li,[1a]* Dong Wang,[1a] Tianjiao Wang,[a] Yang Zhang,[a] Shiyang Liu,[b] Shiwei Zhang,[a] Zhufeng Hu,[a] Liying Li,[a] Guoyong Wang,[a] and Yingmin Zhao[a]

The development of recyclable and self-repairable vitrimer materials featuring reversible B–O bonds has garnered increasing attention. However, their stability and thermomechanical properties remain insufficient for engineering applications in reusable carbon fiber-reinforced composites (CFRCs). Herein, we reported a high-performance epoxy vitrimer containing boronic ester bonds-based dynamic exchange networks, to which a small amount of N-donating imidazole was added for introducing the intermolecular N–B coordination interactions. The obtained vitrimer (**E51-NBO-IMZ**) possessed a high glass transition temperature (T_g) of 198°C and tensile modulus of 3.71 GPa. Compared to the system without imidazole, it exhibited significantly improved solvent resistance due to the stabilization effect of N–B coordination on the B center atoms. Moreover, the stress relaxation tests also indicated a lower activation energy (E_a=151.31 kJ/mol) of **E51-NBO-IMZ** vitrimer, suggesting a better dynamic exchange activity. Despite the high stability and thermomechanical properties, the self-repairing, recycling and degradation of the vitrimer and its CFRCs were successfully achieved under heating, stress or chemical environmental conditions, demonstrating outstanding potentials for practical applications.

1. Introduction

Thermosetting polymer materials and their composites, characterized by low density, superior mechanical properties and exceptional environmental stability, have found extensive applications in the automotive, wind power and aerospace industries.[1-4] Nevertheless, the rapid increase in the usage of thermosetting polymers has engendered significant resource cost pressure and environmental contamination, which was primarily attributable to their inherent non-degradability and non-processability of covalent cross-linked networks.[5-7] To address the above challenges, a novel material featuring covalent adaptable networks (CANs), named as vitrimer, has been developed to construct sustainable polymeric materials and composites with recyclable, processable and repairable properties.[8-13] Hence, Vitrimers were considered as the third category of polymeric materials alongside traditional thermoplastics and thermosets.[14-15] Among them, epoxy vitrimers have garnered the most research attention due to their rich designability, high mechanical performance and application potentials.[16-19]

In recent years, a diverse range of dynamic covalent reactions has been successfully applied in the design and fabrication of CANs based epoxy vitrimers, such as transesterification,[20-22] disulfide exchange,[23-24] imine exchange,[25-27] siloxane exchange,[28-30] Diels–Alder reaction,[31-33] *etc*. Such dynamic chemical bonds can undergo reversible dissociation and reformation under external stimulus (e.g. high temperature, UV radiation, pressure, pH, and catalytic agents), thereby enabling self-healing and rearrangement of the polymeric networks. However, the majority of epoxy vitrimers exhibited certain limitations: First, the initiation of some vitrimers required the incorporation of large amount of catalyst or very high temperature and pressure.[34-35] Besides, the introduction of vulnerable dynamic structures usually led to the weakening of thermal oxygen and chemical stability, as well as mechanical properties.[36-37] These drawbacks have strongly affected the advancement and practical application of epoxy vitrimers. Consequently, it was still a challenge to develop high performance epoxy vitrimers with high mechanical properties, high stability and adequate dynamic capability.

The reversible B–O bonds, mainly synthesized through the dehydration condensation reaction between boronic acids and diols or the trimerization of boronic acids, were an emerging kind of dynamic bonds to construct vitrimers[38-43]. On account of the sensitive sp^2 hybridized electron-deficient boron atoms, they can easily perform reversible dissociation-association reactions without catalyst upon changing of chemical environment and temperature. To date, numerous efforts have been devoted to fabricate B–O bonds-based vitrimers,

a. Aerospace Institute of Advanced Materials & Processing Technology, Beijing, 100074, China.
b. China International Engineering Consulting Corporation, Beijing, 100089, China.
Corresponding author E-mail: liqi032377@163.com

† Electronic supplementary Information (ESI) available. See DOI: 10.1039/x0xx00000x

yet most reported systems were elastomers or low-modulus polymers for the consideration of fast exchange reactions.[44-46] Recently, the use of boronic ester bonds to modify epoxy resins for the construction of high performance vitrimer has been a new research hot-spot. For instance, Zhang et al.[47] reported an epoxy vitrimer based on phenyl boric acid curing agent for green degradation, closed-loop recycling, and ready reprocessing, which exhibited good thermal and mechanical properties. Zeng et al.[48] reported the epoxy networks that were fabricated through the reaction between thiol curing agent containing borate esters and a rosin-derivate containing epoxide group. The epoxy networks displayed effective reprocessing properties with a high recovering degree of mechanical properties. Despite the significant progress in the preparation and dynamic exchange performance of epoxy vitrimers based on B–O bonds, the environmental resistance, thermal resistance, and mechanical properties required further improvement. Moreover, their application in reusable CFRCs needed further verification.

Notably, a series of research have proved that the intra/intermolecular dative N–B interactions gave rise to a structural transformation of boron heterocycles from trigonal planar to tetrahedral, which enhanced the hydrolytic stability of the central boron atom[49-51]. Thus, the formation of N–B coordination can be utilized to promote the stability of boronic ester linkages and confer great mechanical properties of vitrimers. Li et al.[52] reported the study of epoxy resin reacting with a trifunctional amine containing N–B coordinated boronic ester. Owing to the N–B coordinated structure, the dynamically crosslinked epoxy resin possessed good water and humidity resistance. Furthermore, the N–B coordination interaction was reported to be effective to accelerate the dynamics of transesterification of boronic ester and beneficial to the self-healing performance.[53-54] Song et al.[55] reported the synergy between the boronic ester and N–B coordination to improve the mechanical properties and the self-healing efficiency in polyurethanes vitrimers. In this work, the N–B coordination not only accelerated the reshuffling of the boronic ester at room temperature but also dramatically enhanced the mechanical properties.

Herein, we represent an effective strategy for constructing high performance epoxy vitrimer by introducing borate ester-based cross-linking groups and intermolecular N–B coordination (Figure 1). To achieve the fabrication of high-performance epoxy vitrimer, a diamine curing agent containing a pair of borate ester bonds (**NBO**) was designed and synthesized, and used for the cross-linking of typical bisphenol A epoxy monomer (**E51**). In order to introduce the N–B coordination and stabilize the B–O dynamic covalent bonds, a minimal quantity of imidazole (**IMZ**) was added, which concurrently functioned as N-donor and cross-linking reaction accelerator. For comparative analysis, the epoxy vitrimer without imidazole (**E51-NBO**) was also prepared. Characterization results demonstrated that the incorporation of imidazole not only promoted the cross-linking reaction and the glass transition temperature (T_g), but also significantly improved the solvent resistance. Surprisingly, despite the vitrimer with imidazole (**E51-NBO-IMZ**) exhibited superior thermomechanical properties, the stress relaxation test indicated that its activation energy (E_a) was also lower, suggesting a better dynamic exchange activity at elevated temperatures. Taking advantage of the effective B–O bonds-based cross-linking networks, we successfully prepared high performance epoxy vitrimer and its carbon fiber-reinforced composites with excellent recyclability, degradability and self-repairing properties.

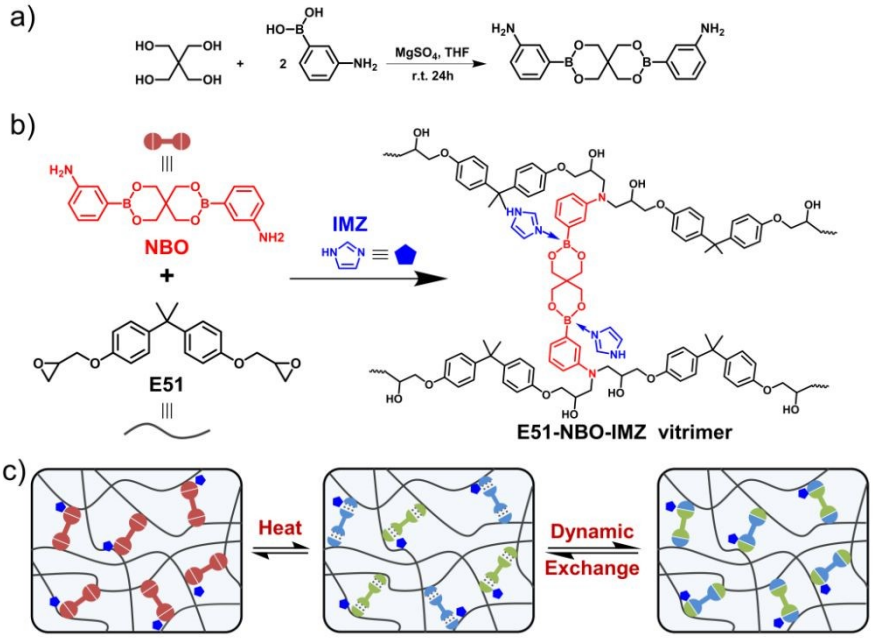

Figure 1. Design concept: a) Synthetic route of B–O bonds-containing diamine curing agent **NBO**; b) Chemical structure of **E51-NBO-IMZ** vitrimer; c) Schematic illustration of the dynamic exchange process of **E51-NBO-IMZ** vitrimer.

View Article Online
DOI: 10.1039/D5LP00144G

ARTICLE

2. Experimental

2.1 Materials

3-aminophenylboronic acid, pentaertyhritol and magnesium sulfate were purchased from Innochem. Analytical pure tetrahydrofuran, dichloromethane, petroleum ether, acetone, ethanol, deionized water, N, N-dimethylformamide and other solvents were commercially available and used as supplied without further purification. The E51 epoxy resin was purchased from Sinopec.

2.2 Characterization

The FTIR spectra were obtained on Nicolet IS10 infrared spectrometer. The solution ^{1}H NMR and solid-state ^{11}B NMR spectra were recorded on a Bruker Avance III 600 spectrometer. The DSC and TGA measurements were carried out on a TA Q200 differential scanning calorimetry. The dynamic mechanical testing was carried out on a TA Q800 dynamic mechanical analyzer. The mechanical property tests were carried out on DDL-100, CSS-44050 and MTS landmark machines. The SEM images were obtained on a JEOL 6390LV instrument.

2.3 Synthesis of borate ester containing curing agent NBO.

Under the protection of nitrogen, 3-aminophenylboronic acid (20 g), pentaerythritol (9.9 g) and magnesium sulfate (64 g) were dissolved in 500 mL of tetrahydrofuran. The reaction solution was stirred at room temperature for 24h. After the reaction was over, the precipitate was removed by filtration, and washed twice by tetrahydrofuran. The organic solution was dried by rotary evaporation to obtain a light-yellow solid. Dichloromethane was added to dissolve the yellow solid under moderate heating, and then petroleum ether was added to for recrystallization. After filtration and drying, 22g of white solid product **NBO** was obtained. The yield was 89%.

2.4 Preparation of E51-NBO vitrimer.

The **E51** epoxy resin and **NBO** curing agent were mixed at a mass ratio of 100:42. The mixture then underwent thorough grinding and dispersion using a three-roll mill. And then the **E51-NBO** prepolymer was placed in a vacuum oven and heated to 60°C under vacuum to eliminate air bubbles. Subsequently, the resin melt was poured into the mold and subjected to a curing process in the oven, following a curing protocol of 120°C/1h-150°C/1h-180°C/1h. Upon natural cooling, the resin casting body of **E51-NBO** vitrimer was obtained.

2.5 Preparation of E51-NBO-IMZ vitrimer.

The **NBO** curing agent and imidazole solid were dissolved in acetone with a molecular weight ratio of 10:1. After stirring at room temperature for 2h, the solution was dried by rotary evaporation to obtain a uniform mixture of **NBO-IMZ**. The material ratio and preparation procedures of **E51-NBO-IMZ** vitrimer were consistent with those of **E51-NBO** vitrimer.

2.6 Preparation of carbon fiber reinforced vitrimer composites.

The **E51-NBO-IMZ** vitrimer prepolymer was dissolved in acetone at room temperature with a solid content of 50%. Upon complete dissolution, the resin solution was uniformly applied onto the carbon fiber fabric by brushing. Upon complete evaporation of the solvent, the vitrimer prepregs were obtained. The carbon fiber reinforced vitrimer composites were fabricated through a mould pressing craft.

3. Results and discussion

3.1 Characterization of E51-NBO and E51-NBO-IMZ vitrimers

In order to improve the heat resistance and mechanical properties of the B–O bonds-based epoxy vitrimers, the **NBO** diamine curing agent with relatively rigid structure and containing a pair of dynamic boronic ester bonds was designed and synthesized. The chemical structure of **NBO** was determined by ^{1}H NMR, ^{13}C NMR and ESI mass spectrum (Figure S1-S3). Through common blending and curing process with **E51** epoxy resin, two kinds of epoxy vitrimers with and without N-donor imidazole were fabricated, respectively named as **E51-NBO-IMZ** vitrimer and **E51-NBO** vitrimer.

The chemical structrues, thermal and mechanical properties of the two vitrimers were characterized and analyzed comparatively. As shown in the FTIR spectra (Figure 2a), the cured **E51-NBO-IMZ** vitrimer and **E51-NBO** vitrimer exhibited similar chemical cross-linking structures. The amino groups in **NBO** cross-linker underwent a ring-opening reaction with the epoxy groups in **E51**. Therefore, in the FTIR spectra of vitrimers, the signals of amino groups at 3433 cm^{-1} and 3359 cm^{-1} disappeared, as well as the signals of epoxy groups at 910 cm^{-1}, indicating the effective cross-linking reactions. In addition, a variable-temperature FTIR spectroscopy was applied to characterize the dynamic exchange properties of the vitrimers (Figure S4), with the increase of temperature, the signals of B–O bonds at around 1305 cm^{-1} and 1430 cm^{-1} had no obvious change on peak shapes and intensity, demonstrating a fast exchange process in vitrimer. The fast exchange feature also contributed to excellent thermo-mechanical properties because of the maintenance of the cross-linked network density.

View Article Online
DOI: 10.1039/D5LP00144G

ARTICLE

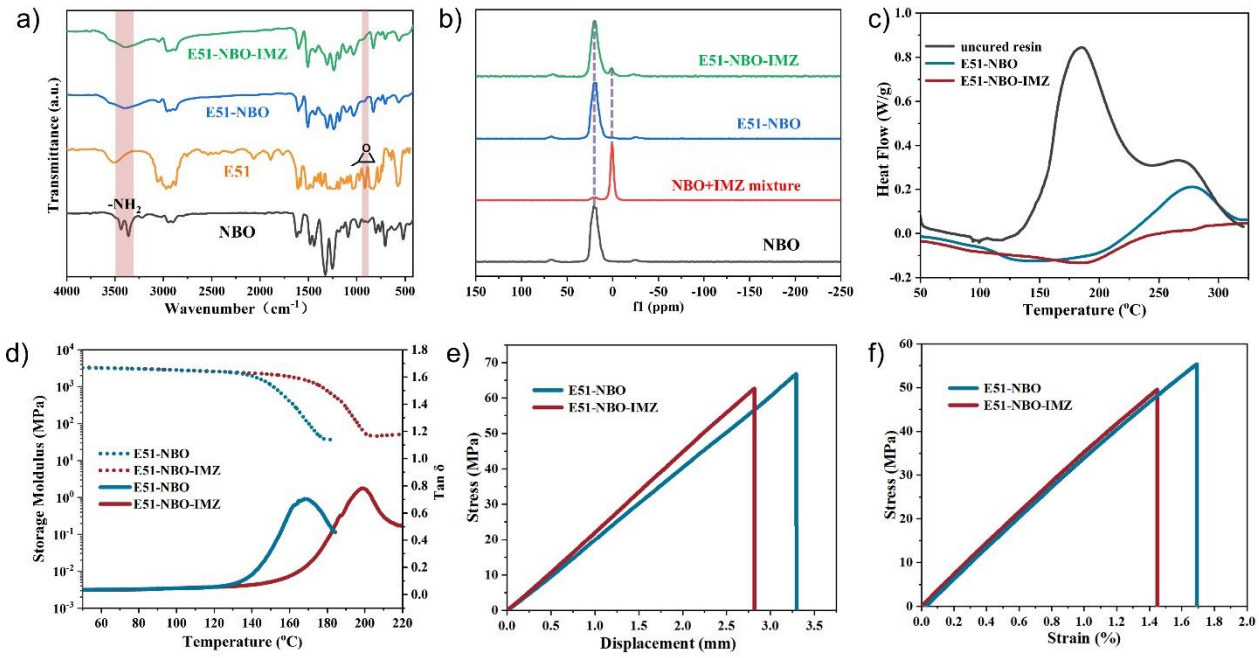

Figure 2. a) FTIR spectra of **NBO**, **E51**, **E51-NBO** vitrimer and **E51-NBO-IMZ** vitrimer; b) Solid-state ^{11}B NMR spectra of **NBO**, **NBO+IMZ** mixture, **E51-NBO** vitrimer and **E51-NBO-IMZ** vitrimer; c) DSC curves of uncured vitrimer, **E51-NBO** vitrimer and **E51-NBO-IMZ** vitrimer. d) DMA curves, e) flexural properties, and f) tensile properties of **E51-NBO** vitrimer and **E51-NBO-IMZ** vitrimer.

To verify the presence of dative N–B interactions in **E51-NBO-IMZ** vitrimer, the solid-state ^{11}B NMR spectroscopy was carried out (Figure 2b). The ^{11}B NMR spectrum of **NBO** showed a single peak at around 20 ppm, which was corresponded to the sp^2 boron atoms in boronic esters. In the equimolar mixture of **NBO** and **IMZ**, the majority of the ^{11}B signals shifted to around 0.8 ppm, which was consistent with the sp^3 boron atoms involving N–B coordination.[56-57] The spectrum of **E51-NBO** vitrimer was nearly the same with that of **NBO**, revealing a similar chemical environment of the boron centers in vitrimer. In the spectrum of **E51-NBO-IMZ** vitrimer, a weak signal peak at 1.0 ppm appeared, demonstrating the N–B coordination in vitrimer upon the addition of **IMZ**.

The Differential Scanning Calorimetry (DSC) analysis was utilized to characterize the residual reaction heat and curing degree. As shown in Figure 2c, the DSC curve of uncured resin showed a broad endothermic peak from 140°C to 300°C. After the curing reaction process, the endothermic peak of the vitrimers significantly decreased. What differs was that the endothermic peak of **E51-NBO-IMZ** vitrimer completely disappeared while **E51-NBO** vitrimer remained a partial endothermic peak at around 250°C. After a post-curing treatment, there was still an endothermic peak in the DSC curve of **E51-NBO** vitrimer (Figure S5). Therefore, it was demonstrated that the addition of **IMZ** accelerator can help enhance the curing reaction activity and increase the cross-linking density, leading to better stability and thermo-mechanical properties.

Following the research on structural characteristics, the thermal properties of **E51-NBO** vitrimer and **E51-NBO-IMZ** vitrimer were measured. According to the DMA results (Figure 2d), **E51-NBO-IMZ** vitrimer exhibited a glass transition temperature (T_g) of 198°C, which was 30°C higher than **E51-NBO** vitrimer (168°C). The much better thermo-mechanical property was attributed to its high-strength cross-linked structure. Despite the significant difference in T_g, the thermo-gravimetric properties of the two vitrimers were essentially identical due to the same monomeric structures (Figure S6).

Flexural and tensile tests were carried out to evaluate the mechanical performance of the two epoxy vitrimers (Figure 2e, 2f). The flexural modulus and strength of **E51-NBO** vitrimer were 3.54GPa and 66.8 MPa, the tensile modulus and strength were 3.71 GPa and 55.2 MPa. On account of the high rigidity, **E51-NBO-IMZ** vitrimer showed a higher flexural moldulus (3.87 Gpa) but lower flexural strength (62.6 MPa). The tensile modulus of **E51-NBO-IMZ** vitrimer was almost the same with **E51-NBO** vitrimer, yet the tensile strength was lower (50.0 MPa) due to the decreased elongation at break.

The test results demonstrated that the mechanical performance of such B–O bond-based epoxy vitrimer systems

View Article Online
DOI: 10.1039/D5LP00144G

was comparable to that of engineering-grade epoxy resin materials, showing the excellent application potentials.[58]

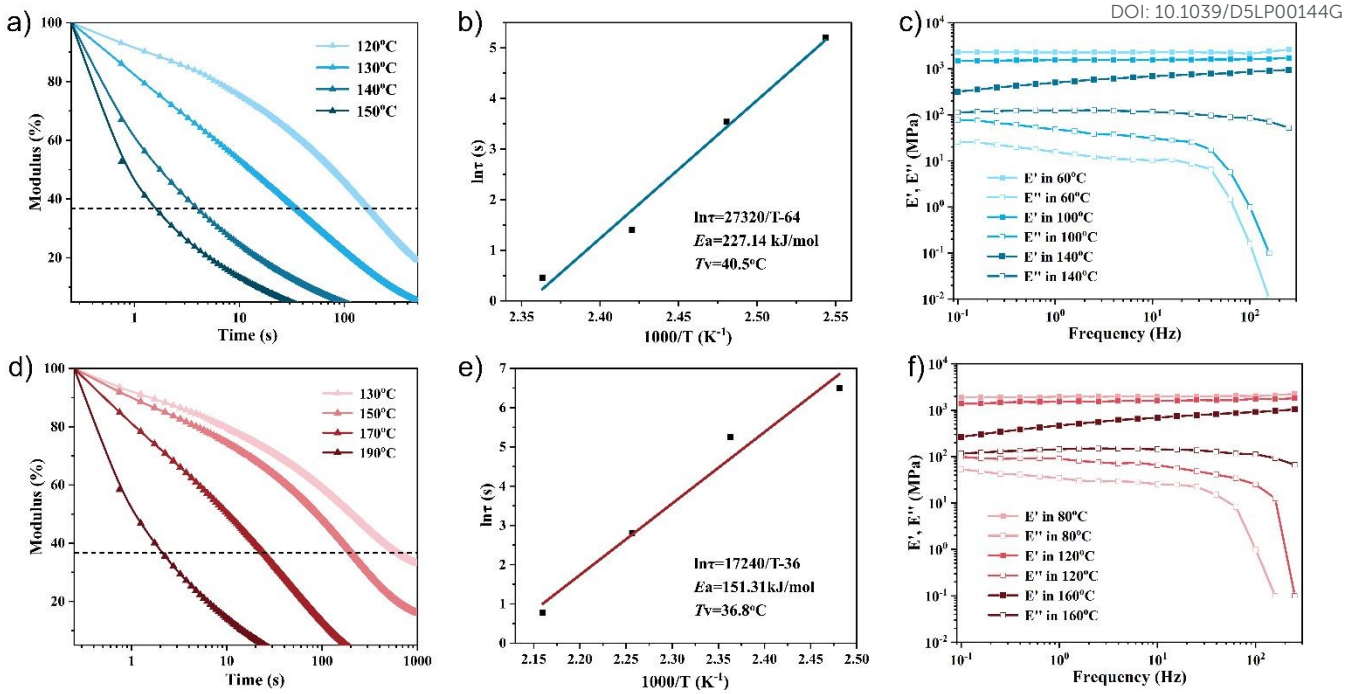

Figure 3. The Stress relaxation curves at various temperatures for a) **E51-NBO** and d) **E51-NBO-IMZ** vitrimers. Linear regression of the logarithm of relaxation time ln(τ) versus reciprocal of temperature (1/T) for b) **E51-NBO** and e) **E51-NBO-IMZ** vitrimers. DMA frequency sweep curves of c) **E51-NBO** and f) **E51-NBO-IMZ** vitrimer under different temperatures.

3.2 Thermally active dynamic properties of E51-NBO and E51-NBO-IMZ vitrimers

The dynamic exchange properties of two vitrimers were investigated through thermally induced stress relaxation experiments. As shown in Figure 3a and 3d, the relaxation rate of the vitrimers significantly accelerated with the temperature increasing. According to the Maxwell model, the relaxation time was defined as the time when modulus reduced to 1/e (i.e., 36.8%) of the initial modulus. The relaxation time (τ) of **E51-NBO** vitrimer at 120°C was 170s, which decreased to 1.6s at 150°C. Due to the high thermo-resistance property, the decrease in relaxation time of **E51-NBO-IMZ** vitrimer required higher temperatures. With temperature increased from 130°C to 190°C, the relaxation time of **E51-NBO-IMZ** vitrimer decreased from 616s to 2.0s. Correspondingly, the variations in creep behavior at different temperatures also confirmed the accelerated dynamic exchange properties (Figure S7).

Based on the results of the stress relaxation experiments, the activation energy (E_a) can be calculated by fitting according to the Arrhenius equation[59-60]:

$$\tau(T)=\tau_0\exp(E_a/RT) \quad (1)$$

Where τ is the relaxation time, E_a is the activation energy, R is the universal gas constant (8.314 J mol^{-1} K^{-1}), and T is the temperature. The linear fitting function of ln(τ) vs 1000/T was shown in Figure 3b and 3e, which indicated that the relaxation times of **E51-NBO** and **E51-NBO-IMZ** vitrimer were in accordance with the Arrhenius's law. The calculated E_a for **E51-NBO** and **E51-NBO-IMZ** vitrimer were 227.14 kJ/mol and 151.31 kJ/mol, respectively, which were higher than published low T_g systems.[61-62] Surprisingly, **E51-NBO-IMZ** vitrimer exhibited a higher T_g but a lower E_a. It was assumed that, on one hand, the higher curing degree of **E51-NBO-IMZ** vitrimer resulted in a higher density of boronic ester dynamic exchange sites in the cross-linked networks. On the other hand, the N–B coordination provided by **IMZ** can help stabilizing the transition state intermediate, thereby accelerating the equilibrium of the dynamic exchange reaction upon heating. In addition to E_a, the topological freezing transition temperature (T_v) was another important parameter to represent the dynamic exchange activity of vitrimers. Referring to the calculation method in the references,[63] the T_v of **E51-NBO** and **E51-NBO-IMZ** vitrimer were determined to be 40.5°C and 36.8°C. This demonstrated that such B–O bond-based vitrimers possessed the nature to dynamically exchange at near room temperature, but the bond exchange reaction was also restricted by the segmental mobility related to T_g. Because of the identical dynamic covalent structures, there was no much difference in T_v between **E51-NBO** and **E51-NBO-IMZ** vitrimer.

The DMA frequency sweep experiments of **E51-NBO** vitrimer and **E51-NBO-IMZ** vitrimer were carried out under different temperatures to test the stability of them in increasing frequencies. Taking into account the difference in T_g of the two vitrimers, the test temperatures of **E51-NBO** vitrimer were 60°C, 100°C and 140°C, while the test temperatures of **E51-NBO-IMZ** vitrimer were 80°C, 120°C and 160°C. As shown in Figure 3c and 3f, with the increase in temperature, the initial storage modulus (E') of two vitrimers decreased and the initial loss modulus (E'') exhibited a slight elevation. At lower temperatures, as the scanning frequency increased, the E' of two vitrimers remained stable, while the E'' sharply dropped to near 0 MPa when the frequency reached above 100 Hz. Compared with **E51-NBO-IMZ** vitrimer, the E'' of **E51-NBO** vitrimer began to decline at lower frequency (40 Hz). When the temperature approached to around topological exchange

temperature of vitrimers, the E' of them gradually increased as the frequency rising, representing the suppression of molecular chain motions at high oscillation frequency and the enhancement of the rigidity. Besides, the E'' of two vitrimers exhibited higher stability under high temperatures. The above experimental results indicated that this kind of epoxy vitrimer had relative stability with respect to frequency but sensitivity to temperature. Furthermore, the addition of imidazole had no significant effect on the frequency responsiveness of the vitrimers.

Furthermore, flexural tests at varying temperatures were applied to characterize the mechanical property variations of **E51-NBO** and **E51-NBO-IMZ** vitrimer under elevated thermal conditions (Figure S8). With the temperature raised from 25°C to 180°C, the modulus of the vitrimers was decreasing at an increasing rapid rate. The modulus of **E51-NBO** vitrimer experienced a sharp decline at 150°C, while **E51-NBO-IMZ** vitrimer was at 180°C. At above 180°C, the modulus of the vitrimers declined to nearly zero, indicating that the deformation and dynamic exchange reactions can effectively occur at around 180°C, which was the foundation for self-repairable and deformable performance under heating conditions.

3.3 Solvent resistance of E51-NBO and E51-NBO-IMZ vitrimers

A series of solvent resistance tests were conducted to characterize and compare the decomposition and swelling performance of **E51-NBO** vitrimer and **E51-NBO-IMZ** vitrimer in different solvents. Considering the sensitivity of the B–O bonds to the protic environments and the vulnerability of epoxy resin to highly polar solvents, we rationally selected four representative solvents: the medium polar protic ethanol, the highly polar protic water, the medium polar aprotic tetrahydrofuran (THF), and the highly polar aprotic N, N-dimethylformamide (DMF). After immersed in solvents for 48h, **E51-NBO** vitrimer and **E51-NBO-IMZ** vitrimer exhibited highly contrasting solvent resistance performance (Figure 4). In medium polar protic ethanol, there were no obvious changes in appearance and volume of the two vitrimers. In highly polar protic water, the outer layer of **E51-NBO** vitrimer block gradually turned white and became rough, with volume slightly increased, indicating that the B–O bonds-based cross-linked structure underwent a slow process of decomposition in water. In highly polar organic solvents THF and DMF, **E51-NBO** vitrimer exhibited significant swelling along with time, and its volume increased to more than double after 48 hours. In DMF, the outer layer was almost dissolved, due to the synergistic effect of swelling and chemical bond decomposition. On the contrary, **E51-NBO-IMZ** vitrimer exhibited little to no change in these solvents after 48h, demonstrating the key role of N–B coordination in enhancing the chemical stability of vitrimer. After about a week, the out layer of **E51-NBO-IMZ** vitrimer exhibited slight swelling, whereas **E51-NBO** vitrimer was almost completely dissolved in DMF (Figure S9).

To characterize the performance after solvent resistance tests, the DMA and flexural test samples of **E51-NBO** and **E51-NBO-IMZ** vitrimers were prepared and placed in different solvents (EtOH, Water, THF and DMF) for 24 hours. After that, the thermal and mechanical properties of the samples were measured. Due to the significant swelling and degradation effect of **E51-NBO** vitrimer in DMF, its samples in DMF were not qualified for the tests. As shown in Figure S10a and S10c, the heat resistance and mechanical properties of **E51-NBO** vitrimer both declined significantly after solvent immersion. Its initial storage modulus exhibited significant decrease and its T_g decreased from 168°C to 164°C (in EtOH), 152°C (in water) and 137°C (in THF), respectively. Meanwhile, its flexural strength and flexural modulus have also decreased significantly, especially for the sample immersed in THF. The decline in thermal and mechanical performance of **E51-NBO** vitrimer was consistent with the results of its solvent resistance test. As for **E51-NBO-IMZ** vitrimer (Figure S10b and S10d), the T_g, flexural strength and flexural modulus were all well maintained, which indicated the excellent solvent resistance performance of B–O bond-based epoxy vitrimer after the addition of imidazole.

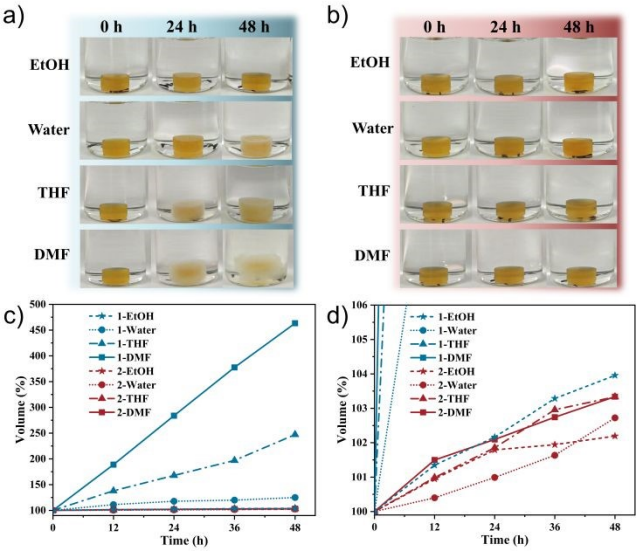

Figure 4. Photographs of a) **E51-NBO** and b) **E51-NBO-IMZ** vitrimers in different solvents for 0h, 24h and 48h. The volume variation over time of c) **E51-NBO** and d) **E51-NBO-IMZ** vitrimers in different solvents.

3.4 Recycling performance of E51-NBO-IMZ vitrimer

Comprehensive performance characterization has proven that the **E51-NBO-IMZ** vitrimer system containing N-donor imidazole possessed superior thermomechanical properties and enhanced stability, thereby presenting greater potential for engineering applications. To validate the feasibility of **E51-NBO-IMZ** vitrimer in recyclable, repairable and degradable epoxy resin-based materials, a series of experiments were carried out.

To verify the recyclability and processability of **E51-NBO-IMZ** vitrimer, the cured vitrimer was smashed into fine particles and underwent a reforming process through hot mould pressing at 180°C and 5 MPa for 1h. The second and third recycled samples were prepared via the same process. To evaluate the retention of mechanical properties of the vitrimer after recycling, the tensile properties of pristine and recycled vitrimer samples were tested. The stress-strain curves were shown in Figure 5b, and the histogram of tensile strength and tensile modulus were shown in Figure 5c. **E51-NBO-IMZ**

vitrimer exhibited monotonously decreased tensile strength as the reprocessing cycles increased. The retention rate of tensile strength was 89% after the first recycling, and reduced to 76% after the third cycle. Nevertheless, there was no significant reduction in the tensile modulus of original and reprocessed vitrimers. The reason why the tensile strength decreased as the number of recycling times increased was that, on the one hand, during the re-molding process after smashing, micro defects or pores gradually accumulated inside the resin, making it prone to failure under load. On the other hand, the epoxy resin underwent a certain degree of aging after repeated hot-pressing. The effect of aging on the tensile strength was relatively significant, while its impact on the tensile modulus was not obvious. The high retention rate of the tensile modulus after multiple cycles was mainly due to the fact that the cross-linking density and rigidity of the vitrimer didn't change significantly after multiple curing processes, which indicated the efficient dynamic exchange and reconstruction of the borate ester bond networks occurred during the recycling process.

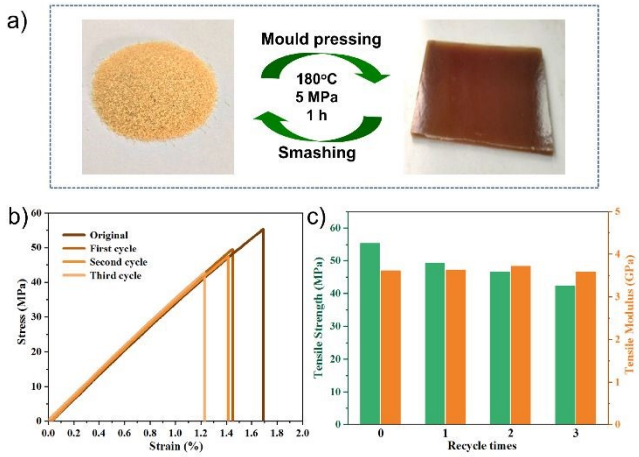

Figure 5. a) Illustration of the recycling and reprocessing of **E51-NBO-IMZ** vitrimer. b) Tensile curves of original and recycled vitrimers. c) Tensile strength and tensile modulus of original and recycled vitrimers.

3.5 Self-repairing performance of E51-NBO-IMZ vitrimer

Taking advantage of the dynamic exchange activity of **E51-NBO-IMZ** vitrimer at high temperature, a series of self-repairing tests on cured vitrimer and CFRCs were conducted. To demonstrate that the self-repair can be achieved under low pressure, a self-repair device based on vacuum bag was designed (as illustrated in Figure 6a). Artificial damages, taking surface scratch and impact cracks as examples, were created on the cured vitrimer samples. Then the samples were placed in the conditions of 200°C and 0.1 MPa vacuum for 10 min. Then the scanning electron microscopy (SEM) and microfocus computed tomography (CT) were employed to characterize the surface morphology and internal quality of the damaged and repaired vitrimer samples. As shown in Figure 6b and 6c, after a short period of softening and chemical bond exchanging under high temperature and vacuum pressure, both the surface and internal defects of **E51-NBO-IMZ** vitrimer have been well repaired. Due to the uneven shaping effect of the peel ply and vacuum bag, corresponding wrinkles and deformations appeared on samples, proving that the plastic deformations effectively occurred on the vitrimer. In contrast, the self-repairing experiments with shorter duration was carried out and showed a partially repaired damage (Figure S11), demonstrating that the defects need sufficient processing time to be fully repaired.

Besides, the self-repair performance of carbon fiber reinforced vitrimer composites was also tested (Figure 6d and 6e). Two kinds of composite specimens respectively with delamination and loose defect were intentionally fabricated, which represented two common types of imperfections encountered during the composite manufacturing processes. Following the same self-repairing procedures, the two defective composite specimens exhibited effective self-repairing capabilities, accompanied by a slight reduction in thickness. In addition, the flexural properties of the CFRC samples before and after self-repairing were measured (Figure S12). The flexural strength and modulus of the loose specimen were both significantly improved after self-repairing. For the delamination defective specimen, the flexural strength was enhanced more significantly. Thus, it is indicated that the CFRCs can achieve efficient self-repair of internal qualities and mechanical properties after the rapid heating and vacuum treatment.

The above experiments demonstrated that **E51-NBO-IMZ** vitrimer and its composites possessed the efficient self-repairing property under high temperature and appropriate pressure, showing the application potential in the field of reusable fiber reinforced composite components.

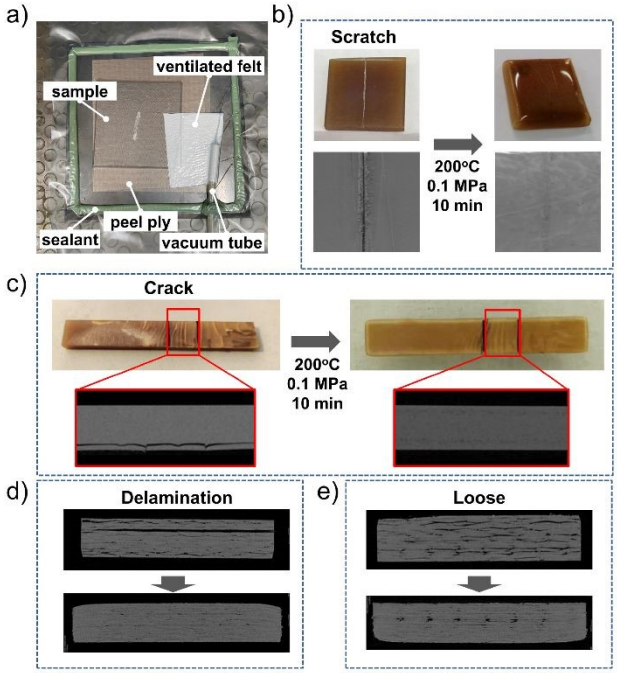

Figure 6. a) Vacuum set-up for self-repairing experiment. b)-e) Characterization before and after the self-repair of damaged **E51-NBO-IMZ** vitrimer and composites.

View Article Online
DOI: 10.1039/D5LP00144G

ARTICLE

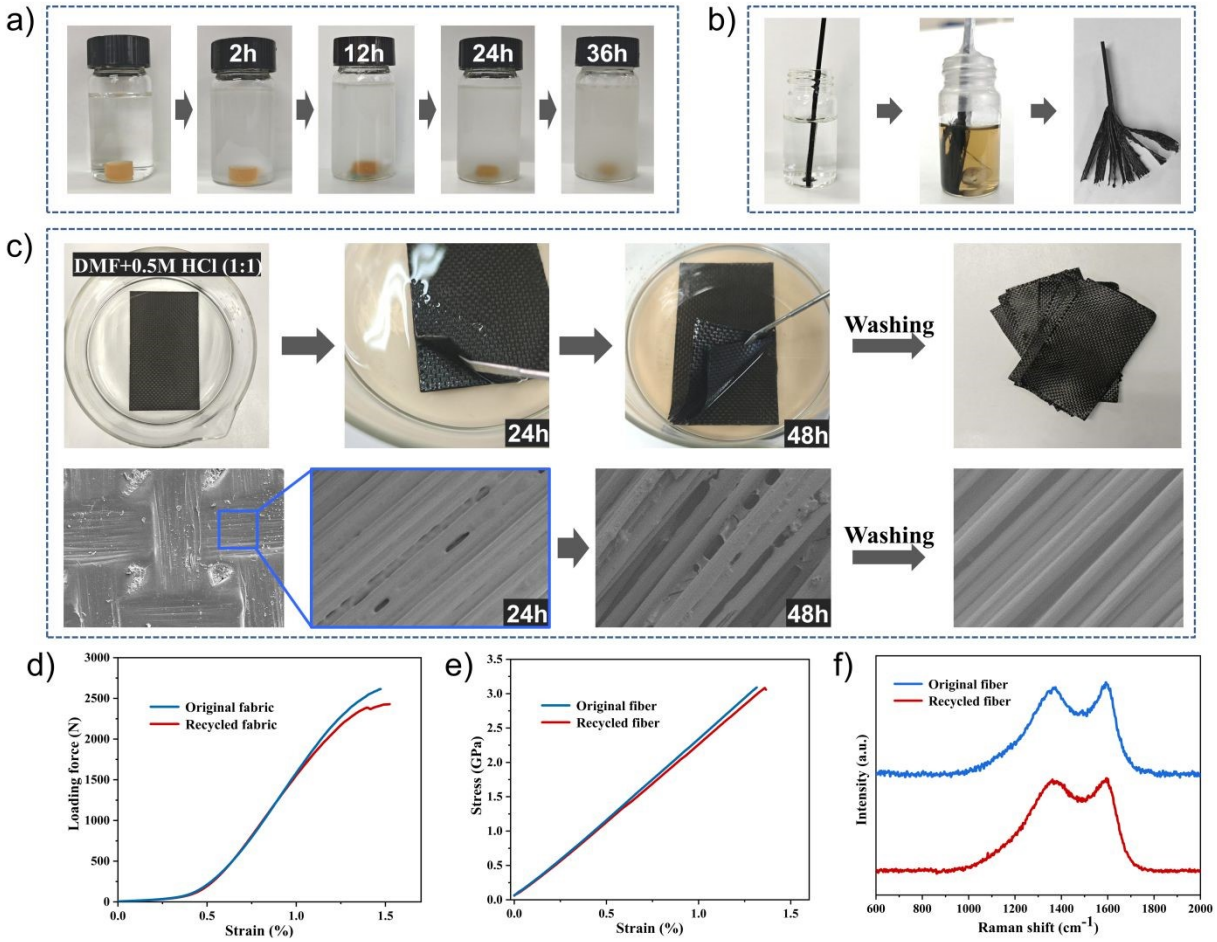

Figure 7. a) Degradation of **E51-NBO-IMZ** vitrimer block in DMF/HCl mixed solvent. b) Degradation of **E51-NBO-IMZ** vitrimer in CFRCs. c) Recycling of carbon fiber fabric in DMF/HCl mixed solvent. d) Fabric tensile curves, e) fiber tensile curves, and f) Raman spectra of original and recycled carbon fibers.

3.6 Degradability and carbon fiber recyclability of E51-NBO-IMZ vitrimer-based composites.

According to the results of the solvent resistance tests, **E51-NBO-IMZ** vitrimer exhibited excellent anti-swelling properties and chemical stability to highly polar and protic environments. This was attributed to the high cross-linking density and dative N–B interactions resulting from the addition of **IMZ**. To verify whether it can degrade in solvents and used as the matrix for the degradable composite materials, we combined polar solvent (DMF) with acidic protonic solvent (HCl aqueous solution) for the degradation experiment of **E51-NBO-IMZ** vitrimer, leveraging the synergistic effect of swelling and B–O bond cleavage.[64-65] The reaction mechanism was that the boronic ester groups in vitrimer can be hydrolyzed into boric acid in an acidic aqueous solution, leading to the dissociation of the cross-linked networks (Figure S13). As shown in Figure 7a, the vitrimer block experienced a gradual dissolution process over time and the solvent became turbid, demonstrating that such a mixed solvent system was practicable for the degradation of **E51-NBO-IMZ** vitrimer. In order to test whether **E51-NBO-IMZ** vitrimer in CFRCs can be effectively degraded, a trip-shaped composite specimen was prepared, of which the lower half was immersed in the same mixed solvent (Figure 7b). After approximately one day, with the assistance of stirring, the immersed part of the composite exhibited significant softening and delamination. After cleaning and drying, the carbon fiber fabric can be easily and completely separated, which verified the feasibility of carbon fiber recycling.

DOI: 10.1039/D5LP00144G

On this basis, a CFRC plate was prepared and immersed in the mixed solvent. The microscopic changes on carbon fibers were characterized by SEM (Figure 7c). After 24 hours, the edges of the composite plate softened and partially delaminated, and the carbon fiber were exposed as the vitrimer on the surface was degraded and dissolved. After 48 hours, the carbon fiber fabric in the composite plate can be easily peeled off layer by layer, and the vitrimer between or inside the carbon fibers also was significantly degraded. Following the cleaning and drying treatment, the carbon fiber fabrics were completely recycled. Moreover, tensile tests and Raman spectroscopy were employed to evaluate the mechanical property and structural quality of the recycle carbon fibers. As shown in Figure 7d and 7e, the modulus and strength of the recycled carbon fiber and fabric were close to those of the original carbon fiber and fabric, but there was a slight decline under high loads. In Raman spectroscopy (Figure 7f), the recycled carbon fiber showed a consistent curves and peak intensities with the original carbon fibers. The I_D/I_G intensity ratio increased from 0.96 to 0.97, representing a very slight increase in carbon fiber defects[66-67]. These phenomena indicated that the **E51-NBO-IMZ** vitrimer based CFRCs can be recycled with the keeping of mechanical properties and structural quality.

4. Conclusions

In summary, a novel borate ester bond-based epoxy vitrimer with improved stability, thermomechanical and thermally activated dynamic exchange properties was constructed and studied. The high epoxy value monomer and high rigidity diamine curing agent containing B–O bonds were employed for the fabrication of high-performance epoxy vitrimer. Besides, a small amount of imidazole was added to introduce the N–B coordination interactions that can stabilize the sensitive B–O bonds. Owing to the promoting effect of imidazole on the epoxy ring opening reaction, **E51-NBO-IMZ** vitrimer exhibited higher cross-linking strength, leading to higher modulus and T_g (198°C). Furthermore, the stress relaxation tests disclosed that **E51-NBO-IMZ** vitrimer had a lower E_a (151.31 kJ/mol), suggesting a better dynamic exchange performance at elevated temperatures. In addition, the dative N–B interactions yielded **E51-NBO-IMZ** vitrimer with remarkable solvent resistance compared to **E51-NBO** vitrimer. The effectively dynamic B–O bonds networks endowed **E51-NBO-IMZ** vitrimer with excellent recyclability, degradability and self-repairing properties under appropriate heating, stress and chemical conditions. All the aforementioned research of N–B coordination enhanced B–O bonds-based vitrimer make it attractive for the fabrication of engineering-applicable high performance vitrimer-based composites. By altering the structure of epoxy monomers and curing agents, a large variety of self-repairing and recyclable epoxy-based composites with pre-designed functions and properties can be generated.

Conflicts of interest

There are no conflicts to declare.

Data availability

All data supporting the findings of this study are within the paper and its supplementary material.

Author Contributions

Qi Li and Dong Wang contributed equally to this work.

Acknowledgements

The authors gratefully acknowledge the support of this research from National Natural Science Foundation (No.51903229 and 52303164).

References

1 V. Schenk, K. Labastie, M. Destarac, P. Olivier, and M. Guerre, *Mater. Adv.,*2022,**3**, 8012–8029.
2 S. Utekar, V. K. Suriya, N. More and A. Rao, C*ompos. Part Eng.*, 2021, **207**, 108596.
3 A. Dorigato, *Adv. Ind. Eng. Polym. Res.,* 2021, **4**, 116–132.
4 D. Montarnal, M. Capelot, F. Tournilhac, L. Leibler, *Science,* 2011, **334**, 965–968.
5 J. Zhang, V.S. Chevali, H. Wang and C.H. Wang, *Composites, Part B*, 2020, **193**, 108053.
6 Y. Yuan, Y. Sun, S. Yan, J. Zhao, S. Liu, M. Zhang, X. Zheng, and L. Jia, *Nat. Commun.,* 2017, **8**, 14657.
7 B. Qin, S. Liu, and J. -F. Xu, *Angew. Chem. Int. Ed.*, 2023, **62**, e202311856.
8 W. Denissen, J. M. Winne, F. E. Du Prez, *Chem. Sci.*, 2016, **7**, 30–38.
9 J.M. Winne, L. Leibler, F.E. Du Prez, *Polym. Chem.,*2019,**10**, 6091–6108.
10 P. Chakma, D. Konkolewicz, *Angew. Chem. Int. Ed.*, 2019, **58**, 9682–9695.
11 Z.P. Zhang, M.Z. Rong, M.Q. Zhang, *Prog. Polym. Sci.,* 2018, **80**, 39–93.
12 T. Yang, X. Lu, X. Wang, X. Wei, N. An, Y. Li, W. Wang, X. Li, X. Fang, and J. Sun, *Angew. Chem. Int. Ed.*, 2024, **63**, e202403972.
13 X. Lu, L. Guo, Y. Wang, and J. Sun, *Adv. Funct. Mater.*, 2025, **35**, 2503106.
14 Y. Wu, Y. Wei, Y. Ji, *Giant*, 2023, **13**, 100136.
15 S. Weidmann, P. Volk, P. Mitschang, and N. Markaide, *Composites, Part A*, 2022, **154**, 106791.
16 P. R. Barnett, J. A. Brackenridge, A. A. Advincula, L. A. Taussig, and D. Nepal, *Composites, Part B*, 2024, **274**, 111270.
17 Y. Zhang, H. Yan, R. Yu, J. Yuan, K. Yang, R. Liu, Y. He, W. Feng, and W. Tian, *Adv. Sci.,* 2023, 2306350.
18 Y. Yang, Y. Xu, Y. Ji, and Y. Wei, *Prog. Mater Sci.*, 2021, **120**, 100710.
19 W. Li, L. Xiao, J. Huang, Y. Wang, X. Nie, and J. Chen, *Compos. Sci. Technol.*, 2022, 109575.
20 Y. Xu, H. Zhang, S. Dai, S. Xu, J. Wang, L. Bi, J. Jiang, and Y. Chen, Compos. Sci. Technol., 2022, **228**, 109676.
21 H. Zhang, and X. Xu, *Composites, Part A*, 2017, **99**, 15–22.
22 K. Yu, Q. Shi, M. L. Dunn, T. Wang, and H. J. Qi, *Adv. Funct. Mater.*, 2016, **26**, 6098–6106.

23 B. Li, G. Zhu, Y. Hao, R. Li, X. Zhang, and X. Guo, *J. Polym. Sci.*, 2024, 1–12.
24 Q. Zhou, X. Zhu, W. Zhang, N. Song, and L. Ni, *ACS Appl. Polym. Mater.*,2020,**2**,1865−1873.
25 J. Xu, W. Sun, Y. Liang, Y. Cheng, and L. Zhang, *Polymer*,2023, **283**, 126233.
26 J. Tellers, R. Pinalli, M. Soliman, J. Vachon and E. Dalcanale, *Polym. Chem.*, 2019, **10**, 5534–5542.
27 W. Denissen, G. Rivero, R. Nicolaÿ, L. Leibler, J. M. Winne and F. E. Du Prez, *Adv. Funct. Mater.,* 2015, **25**, 2451–2457.
28 T. Debsharma, V. Amfilochiou, A. A. Wróblewska, I. De Baere, W. Van Paepegem, and F. E. Du Prez, *J. Am. Chem. Soc.*, 2022, **144**, 12280−12289.
29 M. O. Saed, E. M. Terentjev, *ACS Macro Lett*. 2020, **9**, 749−755.
30 X. Wu, X. Yang, R. Yu, X. -J. Zhao, Y. Zhang, and W. Huang, *J. Mater. Chem. A*, 2018, **6**,10184−10188.
31 B. Strachota, J. Hodan, J. Dybal, and L. Matejka, *Macromol. Mater. Eng.,*2020, **306**, 2000474.
32 K. Sugane, R. Takagi, and M. Shibata, *React. Funct. Polym.*,2018, **131**, 211–218.
33 E. Trovatti, T.M. Lacerda, A.J. Carvalho, A. Gandini, *Adv. Mater.*, 2015,**27**, 2242–2245.
34 X. Kuang, Y. Zhou, Q. Shi, T. Wang, and H. J. Qi, *ACS Sustainable Chem. Eng.* 2018, **6**, 9189−9197.
35 M. Capelot, D. Montarnal, F. Tournilhac and L. Leibler, *J. Am. Chem. Soc.*, 2012, **134**, 7664–7667.
36 X. Zhang, S. Wang, Z. Jiang, and X. Jing, *J. Am. Chem. Soc.* 2020, **142**, 21852−21860.
37 H. Memon, Y. Wei, L. Zhang, Q. Jiang and W. Liu, *Compos. Sci. Technol.*, 2020, **199**, 108314.
38 L. Xie, Y. Wang, G. Chen, H. Feng, N. Zheng, H. Ren, Q. Zhao, and T. Xie, *Compos. Commun.*, 2021, **28**, 100979.
39 O. R. Cromwell, J. Chung, and Z. Guan, *J. Am. Chem. Soc.*, 2015, **137**, 6492−6495.
40 Z. -H. Zhao, C. -H. Li, and J. -L. Zuo, *Smart Mat*. 2023, **4**, e1187;
41 S. Cho, S. Y. Hwang, D. X. Oh, and J. Park, *J. Mater. Chem. A.*, 2021, **9**, 14630–14655.
42 A. P. Bapat, B. S. Sumerlin, and A. Sutti, *Mater Horiz.*, 2020, **7**, 694–714.
43 C. Kim, H. Ejima, and N. Yoshie, *RSC Adv.* 2017, **7**, 19288–19295.
44 C. Bao, Y. -J. Jiang, H. Zhang, X. Lu, and J. Sun, *Adv. Funct. Mater.*, 2018, **28**, 1800560.
45 J. J. Cash, T. Kubo, A. P. Bapat, and B. S. Sumerlin, *Macromolecules*, 2015, **48**, 2098−2106.
46 S. Ito, H. Takata, K. Ono, and N. Iwasawa, *AngewChem.*,2013, **125**, 11251–11254.
47 W. Zhang, Q. Zhou, C. Fang, X. Yuan, X. Li, Q. He, X. Dong, Y. Qi, B. Wang, and W. Li*, J Polym Res,* 2022, **29**, 244.
48 Y. Zeng, J. Li, S. Liu, and B. Yang, *Polymers*, 2021, **13**, 2286.
49 J. Teng, X. Shen, G. Hang, Y. Gao, J. Hu, and S. Zheng, *ACS Appl. Polym. Mater.*, 2025, **7**, 2716−2730.
50 S. Ren, Z. Li, W. Zhou, J. Zhu, Y. Zhao, C. Liu, H. Fang, and Y. Ding, *Ind. Crops Prod.*, 2023, **206**, 117738.
51 W. A. Ogden, and Z. Guan, *J. Am. Chem. Soc.*, 2018, **140**, 6217−6220.
52 Y. Li, Y. Chen, B. Hu, P. Tian, C. Zhang, X. Xing, and X. Jing, *Polymer*, 2025, **329**, 128509.
53 H. Fang, Y. Zhao, X. Xie, F. Zhang, J. Zhu, S. Ren, and Y. Ding, *Polymer*, 2024, **311**, 127587.
54 J. Zheng, Z. Y. Oh, E. Ye, W. H. Chooi, Q. Zhu, X. J. Loh, and Z. Li, *Mater. Chem. Front.*, 2023, **7**, 381–404.
55 K. Song, W. Ye, X. Gao, H. Fang, Y. Zhang, Q. Zhang, X. Li, S. Yang, H. Wei, and Y. Ding, *Mater. Horiz.*, 2021, **8**, 216–223.
56 K. Song, W. Ye, X. Gao, H. Fang, Y. Zhang, Q. Zhang, X. Li, S. Yang, H. Wei, and Y. Ding, *Mater. Horiz.*, 2021, **8**, 216–223.
57 C. Kim, H. Ejima, and N. Yoshie, *J. Mater. Chem. A*, 2018, **6**, 19643–19652.
View Article Online
DOI: 10.1039/D5LP00144G
58 D. Sangaletti, L. Ceseracciu, L. Marini, A. Athanassiou, and A. Zych, *Resour., Conserv., Recycl.*, 2023, **198**, 107205.
59 Y. Fu, S. Chen, X. Chen, H. Zheng, X. Yan, Z. Liu, M. Wang, and L. Liu, *Adv. Funct. Mater.*, 2024, **34**, 2314561;
60 Z. H. Zhao, D. P. Wang, J. L. Zuo, and C. H. Li, *ACS Mater. Lett.*, 2021, **3**,1328–1338.
61 L. Li, J. Xu, Y. Gao, J. Hu, S. Zheng, *React. Funct. Polym.*, 2023, **191**, 105689.
62 Y. Xu, S. Dai, L. Bi, J. Jiang, H. Zhang, Y. Chen, *Chem. Eng. J.*, 2022, **429**, 132518.
63 H. Memon, Y. Wei, L. Zhang, Q. Jiang, and W. Liu, *Chem. Sci. Technol.*, 2020, **199**, 108314.
64 B. Wang, S. Ma, X. Xu, Q. Li, T. Yu, S. Wang, S. Yan, Y. Liu, and J. Zhu, *ACS Sustainable Chem. Eng.*, 2020, **8**, 11162−11170.
65 S. Kumar, and S. Krishnan, *Chem. Pap.*, 2020, **74**, 3785–3807.
66 Z. Jian, Y. Wang, X. Zhang, X. Yang, Z. Wang, X. Lu, and H. Xia, *J. Mater. Chem. A*, 2023, **11**, 21231–21243.
67 Y. -Y. Liu, G. -L. Liu, Y. -D. Li, Y. Weng, and J. -B. Zeng, *ACS Sustainable Chem. Eng.*, 2021, **9**, 4638−4647.

View Article Online
DOI: 10.1039/D5LP00144G

Data availability

All data supporting the findings of this study are within the paper and its supplementary material.